

Article

Anti-Collision System for Small Civil Aircraft

Milan Džunda, Peter Dzurovčin  and Lucia Melníková *

Department of Air Transport Management, Faculty of Aeronautics, Technical University of Košice, 040 01 Košice, Slovakia; milan.dzunda@tuke.sk (M.D.); peter.dzurovcin@tuke.sk (P.D.)

* Correspondence: lucia.melnikova@tuke.sk; Tel.: +42-19-0283-9139

Abstract: This paper presents the results of the research in the field of anti-collision systems for small civil aircraft, which are not dependent on secondary radars and satellite navigation systems. The aviation communication network was used to design the anti-collision system. The simulation results manifested that the anti-collision system precision depended on the errors of synchronization of the aviation communication network. The precision of the anti-collision system is also influenced by the errors of the coordinates of individual aviation communication network users, based on which the system identifies its own position. The results of the simulation show that the dispersion of the positioning error $\sigma^2_{\Delta P}$ by the ACS system varied in the range of 1.94 m² to 503.23 m². The simulation results confirm that the designed anti-collision system is operational in establishing its position against other FOs, with the distance from the given FOs being 50.0 km maximum. The main contribution of this paper are derived algorithms for the operation of an anti-collision system for small civil aircraft, in addition to the design of movement trajectory models of five flying objects which operate within the aviation communication network. The advantage of the anti-collision system is that it is independent of satnav systems and secondary radars. A significant advantage is the low cost of this system.

Keywords: anti-collision system; flying object; accuracy; aviation communication network



Citation: Džunda, M.; Dzurovčin, P.; Melníková, L. Anti-Collision System for Small Civil Aircraft. *Appl. Sci.* **2022**, *12*, 1648. <https://doi.org/10.3390/app12031648>

Academic Editor: Dario Richiedi

Received: 24 November 2021

Accepted: 27 January 2022

Published: 4 February 2022

Publisher's Note: MDPI stays neutral with regard to jurisdictional claims in published maps and institutional affiliations.



Copyright: © 2022 by the authors. Licensee MDPI, Basel, Switzerland. This article is an open access article distributed under the terms and conditions of the Creative Commons Attribution (CC BY) license (<https://creativecommons.org/licenses/by/4.0/>).

1. Introduction

The aviation development affects the growth of air traffic density which may lead to mutual aircraft collisions. In cooperation with ICAO and FAA, European organizations have been dealing with the problems deriving from both the increase and safety of air traffic. NextGen (the USA) and SESAR (the EU) programs together with the ATM/CNS conception have become cornerstones of the future communication infrastructure. The given programs assume that global navigation satellite systems (GNSS) will have a dominant position in all flight phases. Simultaneously, appropriate alternatives are being sought that might serve as a backup in case of GNSS malfunction or breakdown. Great attention is paid to the issue of anti-collision systems (ACS). Most of the published works are devoted to the anti-collision systems of autonomous unmanned aircraft. Very few published works are devoted to the anti-collision system for the category of small aircraft. Some research results in the field of anti-collision systems are presented in [1]. The basic premise of creating an anti-collision system is that all flying objects (FO) work in the aviation communications network and each of the flying objects transmits their location information. An important condition for the operation of the proposed anti-collision system is a synchronous communication network. The design of an onboard anti-collision system for unmanned aerial vehicles (UAVs) is presented in the work [2]. There is an assumption that all UAV work in the communication network and each of the UAVs communicate their location information. It is mentioned in the work, that the basic condition for the operation of the proposed anti-collision system is to work in a common communication network for UAVs. Using the algorithms mentioned in this thesis, it is possible to design the architecture of the anti-collision system for UAV, which can determine its position against other users of the aviation communication network.

The operational economic aspects of detection and anti-collision systems used in helicopters are analyzed in [3]. They listed their helicopter protection anti-collision systems with high voltage wires in the Wire Strike Protection System (WSPS). There is basic information about the Powerline detector provided. Comparing current generations of OASys radar systems (Amphitech Systems) and LOAS (Goodrich Sensor Systems) in terms of their detection performance and financial demands is done to implement them into different types of helicopters. The analyzed accident shows the balance that is directly related to the use of these specific devices on civil helicopters. In the article, we deal with a proposal for an anti-collision system for the small aircraft category. The aircraft of this category essentially perform flights outside of the controlled airspace and their activity is subject to VFR regulations. However, in some instances, a sudden change of weather conditions or an unexpected increase in air traffic may occur. In such situations, it may be difficult for the pilot to see and avoid other airplanes in time as required by the VFR regulations. The pilot would probably appreciate having access to information on the positions of flying objects in the proximity. It would significantly reduce both the time of other aircraft detection and the reaction time needed to take appropriate measures to avoid dangerous situations or collisions. Most small aircraft are equipped with a GPS, nevertheless, their pilots are unable to identify the position of other flying objects in their proximity. As a rule, the anti-collision system is not installed in small aircraft. Only some of them make use of the new ADS-B technology for the monitoring of other aircraft positions in the surroundings. An autonomous system for other aircraft detection in the proximity of a small civil airplane would contribute to the increase of aviation safety. The goal was to propose an anti-collision system for small aircraft capable of providing timely information necessary for effective and safe flights. Such an anti-collision system would be economically advantageous for small aircraft in areas with high-density air traffic as well as areas with a dynamically changing mountainous landscape.

2. Anti-Collision Systems

We distinguish two types of systems—Sense and Avoid (SAA) and See and Avoid (SEA). The See and Avoid principle may be considered a primary method for collision avoiding, in the case of manned aircraft. Each time circumstances allow, pilots are bound to monitor and search for potential conflicts in operations, particularly in the areas where flights are not controlled by an air traffic control (ATC) point.

2.1. Sense and Avoid Systems and Their Use in Small Civil Aircraft

Depending on the technical equipment and characteristics of the targets in proximity, SAA technologies can be divided into cooperative and non-cooperative. There is an option to prescribe the duty of specific equipment on board aircraft but the Sense and Avoid System characteristics usually do not guarantee the possibility of use in all aircraft types. In this case, it is inevitable to broaden the problem to SWAP + PRICE as the additional possibilities of electronics and miniaturizations are significantly broad, but the price of smaller and lighter systems may be much higher. Actively cooperative systems incorporate query devices, and they monitor the sector in front of the flying object. Furthermore, they communicate with the query devices of other aircraft. This kind of system is capable of identifying the direction and distance to the aircraft and it is possible to employ it for flights subject to VFR. The key disadvantage of these systems is their significantly high price. Typical examples are various versions of ACAS systems. Actively non-cooperative systems employ laser or radar sensors to explore the sector in front of the aircraft systematically. The subsequent analysis of a signal reflected from the target makes it possible to calculate the distance, direction, and speed of mutual approaching. Disadvantages of such systems include weight and price. A passive cooperative system takes advantage of the fact that each aircraft automatically transmits its position, speed vector, and speed. In this case, the implemented sensor does not measure anything, it merely calculates the time to the moment of collision based on its speed and position. These systems are substantially

simpler, cheaper, and lighter. Their disadvantage is that in areas with high-density air traffic, interference with their operation may occur. Another disadvantage is that it is impossible to detect targets that do not cooperate.

Passive non-cooperative systems provide elevation and azimuth of surrounding targets. However, the systems are unable to identify the distance or speed of approaching sufficiently. The operation of passive non-cooperative systems is influenced by meteorological phenomena. These systems may be based on camera-like sensors. From the viewpoint of anti-collision technologies safety, it is not possible to employ a single solution as yet. Each technology has its advantages and disadvantages which have to be optimally balanced for a specific type of aircraft. At present, there are several options concerning equipping smaller aircraft with additional systems capable of efficiently operating as anti-collision systems. For the time being, TCAS II system is the only fully accepted anti-collision system of civil aviation and that is why it appears to be the most appropriate candidate for the implementation in this aircraft category as well. On the other hand, its applicability in the category of small aircraft is significantly limited by the financial factor. Other SAA systems are still in an early stage of their development and as such, they are unable to reach the prescribed goals dependably.

2.2. Selected Published Research Results in the Field of Anti-Collision Systems

The algorithms to prevent collisions between various unmanned electrical aerial vehicles (UAV) performing the common goal of moving in the same area are derived in [4]. The condition for these algorithms to work is that all the vehicles are communicating with each other. The results of research work on an anti-collision system with a radar detector of obstacles are discussed in the paper [5]. The main tasks set for this system are the detection of static and moving obstacles, estimation of the distance between an aircraft and an obstacle, as well as their relative velocity. As stated in [6], the 3D laser radar is widely used in unmanned driving systems due to its high precision, strong anti-interference ability, and omni-directional scanning. It is used for anti-collision detection. Its disadvantage is the dependence on the weather. The technology of UAV equipped with a low-power FM ranging radar to construct an anti-collision system is listed in [7]. Radar data analysis and camera image processing are performed to achieve the collision avoidance system. The methods to avoid collisions between a robot and an obstacle, based on distance feedback, was given by a laser Time of Flight (TOF) sensor and are listed in [8]. Two solutions are presented: the former (GCT: Geometry Consistent Trajectory) preserves the geometrical properties of the trajectory, while the latter (TCT: Time Consistent Trajectory) aims at preserving the time properties of the trajectory. The anti-collision function is vital to the UAV [9] to ensure that the UAV can fly more stably and safely. The proposed system can detect surrounding obstacles. The metrological characterization of the infrared distance sensor Teraranger One is given in [10]. A frontal anticollision system based on the sensor in question with the additional functionality of maintaining a fixed distance from the detected target has been suggested. An upgrade of the radar navigation system is listed in [11], particularly, its collision avoidance planning tool. In the paper [12], the anti-collision and obstacle avoidance control of moving sensors for a class of distributed parameter systems with a time-varying delay was investigated. The results of introducing a speed control by using ultrasound and accelerometer sensors to detect objects associated with a fuzzy controller to prevent collisions in enclosed spaces are listed in [13,14]. By implementing this anti-collision model, navigation of aerial robots becomes safer. The study [15] is dedicated to solving a collision prevention task for autonomous unmanned aerial vehicles' team by Immune Neuro-Fuzzy Network (INFN) application. The goal of the research was to develop the machine learning algorithm for autonomous UAV. The improved algorithm for collision prevention based on the combination of immune neural network and fuzzy logic for the team of UAVs is proposed in the paper [16]. The method of calculating the collision probability between agents is listed in [17]. Then, the authors analyze the impact of the position error, the safety radius, and the relative distance on the

collision probability. Despite the value of electronic means of conflict detection (e.g., ACAS and STCA), visual lookout remains an important defense against loss of separation for all classes of aircraft. This is particularly true for pilots of light aircraft, many of which are single-pilot operated, are not equipped with ACAS or transponders, and frequently operate VFR outside ATC radar cover and at low altitudes. These pilots must develop sound visual scanning techniques. To avoid collisions, you must scan effectively from the moment the aircraft moves until it comes to a stop at the end of the flight. Collision threats are present on the ground, at low altitudes in the vicinity of aerodromes, and cruising levels [18]. Researchers at NASA's Armstrong Flight Research Center have dramatically improved upon existing ground collision avoidance technology for aircraft. NASA's system leverages leading-edge fighter safety technology, adapting it to civil aviation use as an advanced warning system. The algorithms have been incorporated into an app for tablet/handheld mobile devices that can be used by pilots in the cockpit, enabling significantly safer general aviation. The advantages of the system include high-fidelity terrain mapping, nuisance-free warnings, multidirectional maneuvers, flexible platforms, and proven technology. The system can be applied in the area of general aviation (personal aircraft), military aircraft (F-16 Fleet), UAVs/drones, helicopters, and digital autopilots [19,20].

3. Design of the Anti-Collision System for the Category of Small Aircraft

Based on the conducted analysis of the accessible methods of flying objects position identification, the conclusion is that the distance measuring method would be the most appropriate for the design of the architecture of an anti-collision system for small civil aircraft. We assume that the proposed system will operate in the communication network of aviation. The European Commission's directive maintains that the category of small aircraft up to 5700 kg do not have to be equipped with a certified anti-collision system ACAS II. Implementation of the offered versions of these systems onboard aircraft involves significant financial expenses. On the other hand, their absence has a direct influence on the safety of air traffic operations. The aim is to design an appropriate equivalent of the currently employed anti-collision systems which will be usable for the category of small aircraft.

Model of Anti-Collision System

The designed model assumes that all flying objects operate in the communication network of aviation and each flying object transmits information on its position. Another prerequisite for the operation of the anti-collision system designed by us is that the communication network must be synchronized. Every user is given a strictly specified time for the transmission of communication messages. Designing the anti-collision system, we started from the fact that if we know the location of a minimum of four points in the space and the distances of these points from an unknown point, we can calculate the position of the unknown point. In case we presuppose that based on message transmission by individual network users, the anti-collision system will know the location of those users. It will also be able to measure distances from those users because individual users will provide times of communication message transmissions. This method of position determining is a designated telemetric method. The principle of the telemetric method is described in detail in [1,2]. In aviation, location is usually being expressed in geographical coordinates in WGS-84. Designing the anti-collision system, the rectangular Earth-Centered, Earth-Fixed coordinate system (ECEF) is used. Let us suppose that all users in the communication network in Figure 1 transmit in short time intervals, among other things, messages on their positions. The time of signals spreading from one user to the anti-collision system is directly proportional to the distance between that system's receiver and the source of transmission (ST). Measuring the distances of more users of the aviation communication network from the anti-collision system is possible to determine their location. The position of the anti-collision system P against other users of communication network $P_i t_i$, $i = 1$ to 4 , is demonstrated in Figure 2.

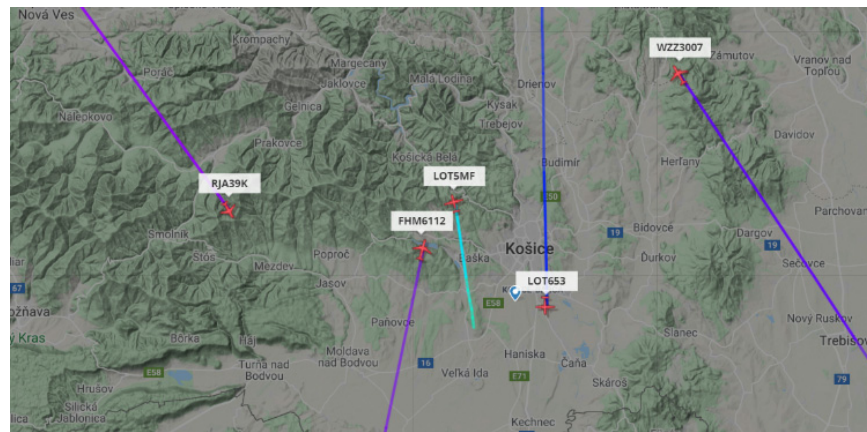


Figure 1. Position of aircraft in the airspace according to flightradar24.

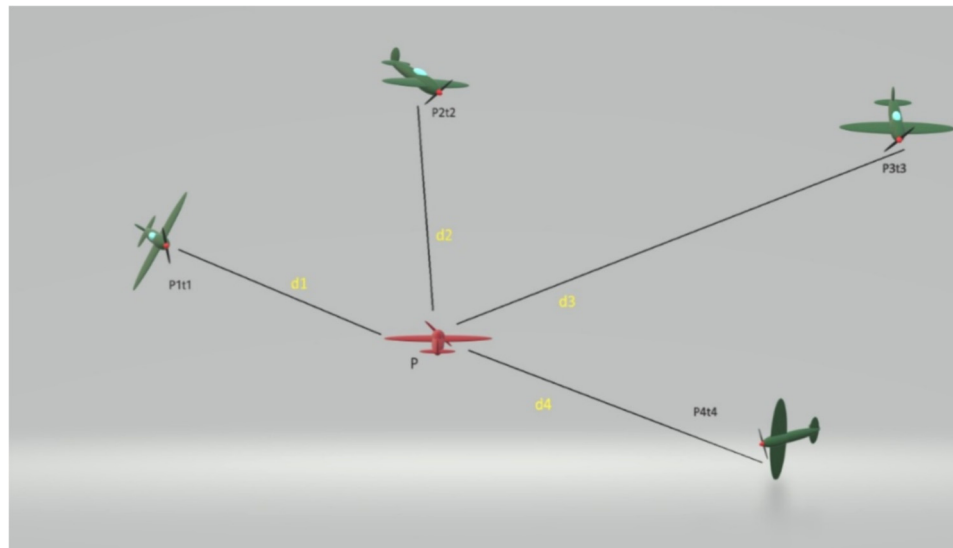


Figure 2. Position of the anti-collision system P concerning other users of the communication network.

Figure 1 reflects an air situation in the aviation communication system. The used symbols:

P—position of the aircraft with the anti-collision system;

P_{1–4}—positions of other users 1–4 in the communication network;

t_{1–4}—times at which messages were sent;

d_{1–4}—distances of users from the anti-collision system.

On condition that we have identified the coordinates of individual users of the aviation communication network (x_i, y_i, z_i) and the distances of the anti-collision system from those users, we can determine its position P with the coordinates x, y, z :

$$d_i = \sqrt{(x - x_i)^2 + (y - y_i)^2 + (z - z_i)^2}, \text{ where } i = 1, 2, 3, 4 \quad (1)$$

If the user P_i sends the message at the time t_i, the message will be received at the time t_p. Provided that the speed of electromagnetic waves spreading (c) is known, the distance between the source of transmission and the receiver of the user d_i is as follows:

$$d_i = c(t_{pi} - t_i) = c\tau_i \text{ where } i = 1, 2, 3, 4 \quad (2)$$

The calculated distance is burdened with several errors. For that reason, the distance is denoted pseudo-distance. If the time base of the user’s receiver P_i is shifted by an unknown time interval Δt , then this interval can be converted to a distance b using the equation:

$$b = c.\Delta t. \tag{3}$$

The actual distance then will be equal:

$$D_i = d_i - b \tag{4}$$

where: d_i —measured pseudo-distance, D_i —actual distance, b —error of distance measurement. The delay Δt causes a distance D_i measurement error due to a shift in the time bases of the flying objects and the anti-collision system.

The unknown coordinates of the user include the unknown b and to calculate the position we need four equations of the following form:

$$(d_i - b) = c.(\tau_i - \Delta t) = \sqrt{(x - x_i)^2 + (y - y_i)^2 + (z - z_i)^2} \tag{5}$$

where $i = 1, 2, 3, 4$

After adjustments we get:

$$(x - x_i)^2 + (y - y_i)^2 + (z - z_i)^2 - (b - d_i)^2 = 0, \text{ where } i = 1, 2, 3, 4 \tag{6}$$

x, y, z —position of the anti-collision system’s receiver;

d_i —measured pseudo-distance from the anti-collision system to i th user;

τ_i —time of the signal spreading from the i th user to the anti-collision system $P(x, y, z)$;

Δt —time interval by which the receiver’s time base is shifted;

b —a shift of the receiver’s time base converted into distance.

The position of the anti-collision system’s receiver will be expressed through four equations in four unknowns:

$$(x - x_1)^2 + (y - y_1)^2 + (z - z_1)^2 - (b - d_1)^2 = 0, \tag{7}$$

$$(x - x_2)^2 + (y - y_2)^2 + (z - z_2)^2 - (b - d_2)^2 = 0, \tag{8}$$

$$(x - x_3)^2 + (y - y_3)^2 + (z - z_3)^2 - (b - d_3)^2 = 0, \tag{9}$$

$$(x - x_4)^2 + (y - y_4)^2 + (z - z_4)^2 - (b - d_4)^2 = 0, \tag{10}$$

where:

d_1, d_2, d_3, d_4 —measured pseudo-distances from P_{1-4} to the anti-collision system’s receiver;

x_1, y_1, z_1 —coordinates of the user P_1 ;

x_2, y_2, z_2 —coordinates of the user P_2 ;

x_3, y_3, z_3 —coordinates of the user P_3 ;

x_4, y_4, z_4 —coordinates of the user P_4 ;

x, y, z —coordinates of the anti-collision system’s receiver;

b —a shift of the receiver’s time base converted to distance.

For subtraction of Equations (10) from (7), is valid:

$$f_{14} = x_{14}x + y_{14}y + z_{14}z + d_{41}b + e_{14} \tag{11}$$

For subtraction of Equation (6) from (3), is valid it holds:

$$f_{24} = x_{24}x + y_{24}y + z_{24}z + d_{42}b + e_{24} \tag{12}$$

For subtraction of Equation (6) from (4), the following is valid:

$$f_{34} = x_{34}x + y_{34}y + z_{34}z + d_{43}b + e_{34} \tag{13}$$

If variable b is considered as constant (the so-called factor of homogenization), then, depending on Equations (11)–(13), a system of three equations with three unknown variables was obtained. The method of resultants of the multi-polynomials is applied to solve the system of linear equations $x = g(b)$, $y = g(b)$, $z = g(b)$ [21].

The following is valid:

$$f_1 = (x_{14}x + d_{41}b + e_{14})k + y_{14}y + z_{14}z \tag{14}$$

$$f_2 = (x_{24}x + d_{42}b + e_{24})k + y_{24}y + z_{24}z \tag{15}$$

$$f_3 = (x_{34}x + d_{43}b + e_{34})k + y_{34}y + z_{34}z \tag{16}$$

If the variable “ k ” turns into the factor of homogenization, Jacobi’s determinant of the coordinate x by (14), (15), (16) is expressed as:

$$J_x = \det \begin{pmatrix} \frac{df_1}{dy} & \frac{df_1}{dz} & \frac{df_1}{dk} \\ \frac{df_2}{dy} & \frac{df_2}{dz} & \frac{df_2}{dk} \\ \frac{df_3}{dy} & \frac{df_3}{dz} & \frac{df_3}{dk} \end{pmatrix} = \det \tag{17}$$

In compliance with Equations (14–16), for $y = g(b)$ is valid:

$$f_4 = (y_{14}y + d_{41}b + e_{14})k + x_{14}x + z_{14}z \tag{18}$$

$$f_5 = (y_{24}y + d_{42}b + e_{24})k + x_{24}x + z_{24}z \tag{19}$$

$$f_6 = (y_{34}y + d_{43}b + e_{34})k + x_{34}x + z_{34}z \tag{20}$$

Jacobi’s determinant for the coordinate y is expressed as:

$$J_y = \det \begin{pmatrix} \frac{df_4}{dx} & \frac{df_4}{dz} & \frac{df_4}{dk} \\ \frac{df_5}{dx} & \frac{df_5}{dz} & \frac{df_5}{dk} \\ \frac{df_6}{dx} & \frac{df_6}{dz} & \frac{df_6}{dk} \end{pmatrix} = \det \tag{21}$$

In compliance with Equations (14–16), for $z = g(b)$ is valid:

$$f_7 = (z_{14}z + d_{41}b + e_{14})k + x_{14}x + y_{14}y \tag{22}$$

$$f_8 = (z_{24}z + d_{42}b + e_{24})k + x_{24}x + y_{24}y \tag{23}$$

$$f_9 = (z_{34}z + d_{43}b + e_{34})k + x_{34}x + y_{34}y \tag{24}$$

Jacobi’s determinant for coordinate z is expressed as:

$$J_z = \det \begin{pmatrix} \frac{df_7}{dx} & \frac{df_7}{dy} & \frac{df_7}{dk} \\ \frac{df_8}{dx} & \frac{df_8}{dy} & \frac{df_8}{dk} \\ \frac{df_9}{dx} & \frac{df_9}{dy} & \frac{df_9}{dk} \end{pmatrix} = \det \tag{25}$$

From Equations (17), (21) and (25), the value of the determinants J_x , J_y , J_z was obtained. The variable equations $x = g(b)$, $y = g(b)$, $z = g(b)$ by applying the value of each determinant

are the results. Substituting the expression for x, y, z into the Equation (2), the quadratic function for the unknown variable b is obtained:

$$Ab^2 + Bb + C = 0 \tag{26}$$

Solutions of the quadratic Equation (21) have two roots, b_+ and b_- . Calculate the coordinates of the FO (x_+, y_+, z_+) and P (x_-, y_-, z_-). Come to the correct solution, calculate the norm ($norm = \sqrt{x^2 + y^2 + z^2}$) for (x, y, z) b_- and (x, y, z) b_+ . If the coordinates of the receiver are fed into the coordinate reference system, the norm of the position vector will be close to the value of the radius of the Earth ($R_e = 6,372,797$ km) and this solution for the FO (x, y, z) is regarded as a correct one [21].

4. Accuracy of Determining the Position of Flying Objects by Anti-Collision System

According to the derived Equations (1) to (26), the operation of the anti-collision system was simulated, and the accuracy of determining the position of flying objects with this system was evaluated. The influence of the position of flying objects on the accuracy of the anti-collision system was monitored. The individual test examples were designed to examine the ability of the anti-collision system to determine the position of flying objects around an aircraft with sufficient accuracy. The selected simulation results are shown in Figures 3–10.

4.1. Verification of the Functionality of Derived Algorithms

To simulate the operation of the anti-collision system, five FOs motion models in three-dimensional space were created. We chose the initial positions of the FOs to correspond to the real operation in the airspace according to flightradar24. Based on the observation of the movement of aircraft over the territory of the Slovak Republic, there were randomly selected five aircraft and their coordinates were found out at a given time. Since the data come from GPS, it is determined by latitude, longitude, and altitude according to WGS-84. Figure 3 shows a random selection of four transmission sources (aircraft) with a known position and the fifth aircraft, highlighted in red, on which the anti-collision system is located. The position of this aircraft was calculated by applying algorithms that were created during the research which verifies the correctness of the solution. In Tables 1 and 2, the initial position of the selected FOs is listed. In the following simulations, it is assumed that the anti-collision system is located on FO LOT5MF.

Table 1. Initial coordinates of users by flightradar24.

S.n.	Identification	Lat. (° sš)	Long. (° vd)	Lat. (Rad)	Long. (Rad)	Height ASL (m)
1.	RJA39K	48,720	20,869	0.850324	0.364233	11,262
2.	FHM6112	48,758	21,119	0.850988	0.368596	10,683
3.	LOT653	48,633	21,289	0.848806	0.371563	7003
4.	WZZ3007	48,916	21,442	0.853745	0.374233	10,363
5.	LOT5MF	48,771	21,148	0.851215	0.369102	3784

Table 2. Initial coordinates in JTSK.

S.n.	Identification	X (km)	Y (km)	Z (km)
1	RJA39K	3946.254	1504.482	4778.536
2	FHM6112	3936.328	1520.402	4780.893
3	LOT653	3939.279	1534.99	4768.94
4	WZZ3007	3915.165	1537.648	4792.236
5	LOT5MF	3930.301	1520.361	4776.659

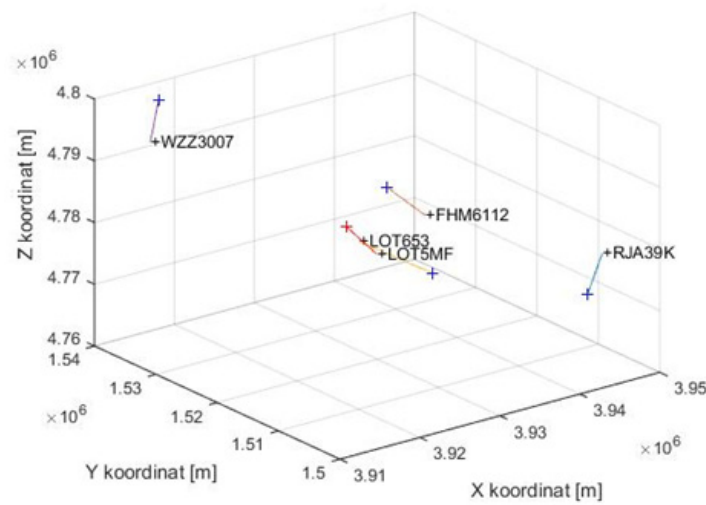


Figure 3. FOs’ flight trajectories for straight flights.

The selected situation corresponds to real air traffic. An anti-collision system is located on board the LOT5MF, which, based on the received messages regarding the positions of other FOs, can detect the surrounding traffic and determine the aircraft’s position. The created model of the anti-collision system by simulation was verified. Based on algorithms, the position of LOT5MF was calculated. In the calculation, the initial coordinates LO from Table 1 and 2 are used. The assumption is that the undulation of the geoid is 40.0 m.

Table 3 shows the LOT5MF coordinates, calculated using algorithms. The calculations confirmed that the derived algorithms are correct. After verifying the correctness of the algorithms for position calculation, we can proceed to the visualization of models of movements of the users.

Table 3. The initial position of FO was obtained by calculation according to derived algorithms.

ID	X (km)	Y (km)	Z (km)	Lat. (°)	Long. (°)	Height ASL (m)
LOT5MF	3930.301	1520.361	4776.659	48.7712N	21.1476E	3784

The FO flight trajectory model is designed to verify the accuracy of the anti-collision system. Based on the created FO models, information about their geocentric position in space can be obtained. Abstracting from the forces acting on the FO during the flight, to simulate anti-collision systems, this fact can be considered irrelevant. The methodology for creating flight trajectory models of FOs is analyzed in detail in [22]. The initial coordinates of the FOs are determined according to flightradar24 in geographical coordinates (LLH). See Table 1. When modeling FOs’ trajectories, each part of their trajectory is modeled in a geocentric coordinate system (ECEF). See Figure 4. Therefore, it was necessary to transform the initial coordinates of the FOs into a geocentric coordinate system (Table 2). Five models of straight flight trajectory FOs and five models of flight trajectories with maneuvers were created, which consisted of straight flight and two turns. Based on this, it is possible to evaluate the accuracy of the anti-collision system during straight flight and FO maneuvers. The input parameters of the flight trajectory model, which can be changed according to current requirements, are the initial position of the FO, the time of straight flight or flight in turns, the flight speed, and the radius of curvature. After performing the simulation, we can visualize the FO motion model in the ECEF system. The position of FOs is determined by the coordinates x_i , y_i , and z_i , $i = 1$ to 5, in meters. The straight flight model lasted 1375.0 s. The flight speed of the flying objects was $100 \text{ m}\cdot\text{s}^{-1}$. We used the equation of a line in three-dimensional space. We assume that the line is uniquely given by two points or one point and a direction vector. The initial coordinates of the FOs’ flight trajectories are given in Table 2. The flight altitudes were constant. The initial coordinates of the FOs in

Figure 3 are marked with a black (+) sign and the FO identification mark. When modeling FO₁₋₅ motion, row matrices are created in Matlab:

$$FO_i a = [a_1^i, a_2^i, \dots, a_n^i]; FO_i b = [b_1^i, b_2^i, \dots, b_n^i]; FO_i c = [c_1^i, c_2^i, \dots, c_n^i] \quad (27)$$

where: $i = 1, 2, 3, 4, 5$ (number of FOs); n —flight time FO _{i} in seconds; $a_1^i, a_2^i, \dots, a_n^i$ —coordinate x of the i -th user FO _{i} ; $b_1^i, b_2^i, \dots, b_n^i$ —coordinate y of the i -th user FO _{i} ; $c_1^i, c_2^i, \dots, c_n^i$ —coordinate z of the i -th user FO _{i} .

Subsequently, we created models of the flight trajectory of five FOs with a maneuver, which consists of a straight flight and two turns. When creating this model, we assume that the flying object flies at a constant altitude. The first section is a straight line and lasts 375 s. The next two sections contain two turns, each lasting 500 s. The initial coordinates of the FOs are identical to the first case in straight flight. The trajectories of the movements of the five FOs for the maneuverer flight are shown in Figure 4.

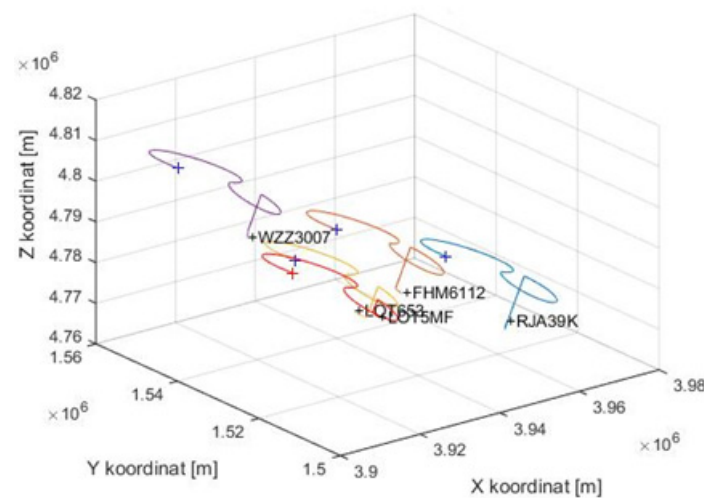


Figure 4. FOs' flight trajectories for maneuverer flight.

4.2. Methodological Error of the Anti-Collision System

In further considerations, we assume an ideal situation where the receiver of the anti-collision system receives from flying objects the exact values of their coordinates FO _{i} a , FO _{i} b , and FO _{i} c . Based on the measurement, it determines the exact values of distances, d_{1-4} . See Figure 2. Following Equations (1) to (27), a simulation of the positioning of the user LO₅ with the anti-collision system for a straight flight was performed (see Figure 3). The simulation results are shown in Figure 5.

Figure 5 shows the errors in determining the coordinates of the anti-collision system ΔX , ΔY , and ΔZ , and also the positioning error ΔP of the anti-collision system. The positioning error ΔP of the anti-collision system is defined as the distance between the actual and measured position of the anti-collision system. The figure shows that the errors in determining the coordinates ΔX , ΔY , and ΔZ of the anti-collision system are in the range of $\pm 5.0 \times 10^{-9}$ m. The positioning error of the anti-collision system varies in the range of 0 to 1.0×10^{-5} m. The mean value of the positioning error of the anti-collision system ΔP is equal to 0.8×10^{-7} m. The dispersion of the positioning error of the anti-collision system is equal to 0.7×10^{-12} m². The simulation results have confirmed that the derived algorithms for the positioning of FOs show a methodological error, which can be neglected due to the required accuracy of positioning by the anti-collision system. In the next step, following algorithms, another simulation of the flight trajectories of five FOs was performed for a maneuverer flight (see Figure 4) under the same conditions as in a straight flight. The results of this simulation are shown in Figure 6.

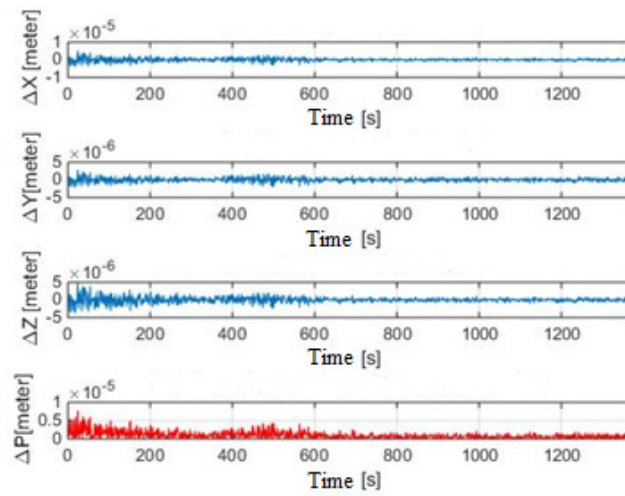


Figure 5. Coordinate determination errors ΔX , ΔY , ΔZ , and position ΔP , straight flight.

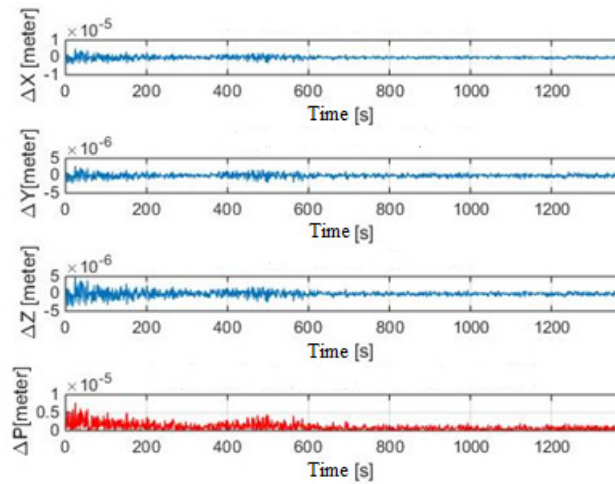


Figure 6. Coordinate determination errors ΔX , ΔY , ΔZ and position ΔP , flight with the maneuver.

The figure shows that the errors in determining the coordinates ΔX , ΔY , and ΔZ of the anti-collision system are in the range of $\pm 1.0 \times 10^{-9}$ m. The mean value of the positioning error of the anti-collision system ΔP is equal to 0.1×10^{-5} m. The dispersion of the positioning error of the anti-collision system is equal to 0.9×10^{-12} m². The results of both simulations confirmed that the derived algorithms for determining the position of the anti-collision system show approximately the same methodological error, which, given the required accuracy of positioning by the anti-collision system, can be considered negligible. Based on the simulation results, Equations (1) to (27) can be used to design an anti-collision system for small civil aircraft.

4.3. Methodology for Evaluating the Accuracy of the Anti-Collision System

The assessment of the accuracy of the anti-collision system needs to be carefully analyzed. The main sources of possible errors include the geometric configuration of the communication network users, the quality of the parameters transmitted in the FOs' position report, and the network synchronization. The task is to assess the effect of distance measurement errors Δd_{1-4} on the determination of the position of the anti-collision system. In the simulations, the distance measurement errors Δd_{1-4} with a random number generator with a normal distribution are mimicked. The generated random numbers are added to the actual coordinates FO_{1-4} . The parameters of the normalized normal distribution are as follows: $E(x) = m = 0$ is the mean and the variance $V(x) = \sigma^2 = 1$. As detected,

pseudo-distances from four broadcast sources and 12 random number generators are available. To set the size of the error, the constant k, multiplied by each generated number is used, where:

$$M[k.X] = k. M. [X] \tag{28}$$

$$D[c.X] = c^2. D[X], \tag{29}$$

where: M—mean value, D—dispersion, k—non-random variable (constant), X—random variable.

The created program writes errors to the row matrix for each coordinate and each user separately:

$$X_{LOi} = [\Delta x_1^i, \Delta x_2^i, \dots, \Delta x_n^i], \tag{30}$$

$$Y_{LOi} = [\Delta y_1^i, \Delta y_2^i, \dots, \Delta y_n^i], \tag{31}$$

$$Z_{LOi} = [\Delta z_1^i, \Delta z_2^i, \dots, \Delta z_n^i], \tag{32}$$

where: i = 1,2,3,4 (user index);

n is the length of the flight in seconds;

X_{LOi}—row matrix of randomly generated errors of x coordinate of user FO_i;

Y_{LOi}—row matrix of randomly generated errors of y coordinate of user FO_i;

Z_{LOi}—row matrix of randomly generated errors of z coordinate of user FO_i.

Using the scalar sum operation of matrix elements (27) and matrix elements (30) to (32), we obtain new row matrices, the elements of which represent the X, Y, Z coordinates of each FO with error.

$$LOi X = FOia + XLOi = [a_1^i + \Delta x_1^i, a_2^i + \Delta x_2^i, \dots, a_n^i + \Delta x_n^i], \tag{33}$$

$$LOi Y = FOib + YLOi = [b_1^i + \Delta y_1^i, b_2^i + \Delta y_2^i, \dots, b_n^i + \Delta y_n^i], \tag{34}$$

$$LOi Z = FOic + ZLOi = [c_1^i + \Delta z_1^i, c_2^i + \Delta z_2^i, \dots, c_n^i + \Delta z_n^i], \tag{35}$$

where:

LOi X—row matrix of coordinate X of user FO_i with error Δ xⁱ;

LOi Y—row matrix of coordinate Y of user FO_i with error Δ yⁱ;

LOi Z—row matrix of coordinate Z of user FO_i with error Δ zⁱ.

To calculate the pseudo-range to an unknown user LO₅ with ACS, the geocentric coordinates from Equation (27) and the coordinates of other users FO₁₋₄ from matrices (33) to (35) will be used. Following Equation (1), the equation for calculating the pseudo-range Δd_i is obtained:

$$d_i = \sqrt{(a_{1...n}^5 - (a_{1...n}^i + \Delta x_{1...n}^i))^2 + (b_{1...n}^5 - (b_{1...n}^i + \Delta y_{1...n}^i))^2 + (c_{1...n}^5 - (c_{1...n}^i + \Delta z_{1...n}^i))^2} \tag{36}$$

where: i=1,2,3,4, (user index); a_{1...n}⁵, b_{1...n}⁵, c_{1...n}⁵—coordinates x, y, z of user FO₅ with ACS at time n.

The distance measurement error Δd_i is as follows:

$$\Delta d_i = D_i - d_i \tag{37}$$

where: D_i—the actual distance between FO_i, and ACS d_i—calculated pseudo-distance between FO_i and ACS.

4.4. Discussion and Results of Anti-Collision System Accuracy Evaluation

In order to verify the sensitivity of the proposed algorithms to inaccuracies in measuring the distance of FO₁₋₄ network users from ACS, we performed additional simulations for a straight flight of 1375 s and also for a flight with a maneuver of 1375 s. The maneuver flight contained two turns, each lasting 500 s. The initial coordinates of the FOs are given in Tables 1 and 2. In this simulation, the errors are added which are generated by the

12 random number generators to the exact coordinates of the FO₁₋₄ users. This simulates the inaccuracies of the distance measurement from all network users to the ACS. The magnitude of the distance measurement inaccuracy is changed using the constant k following Equations (28) and (29). The constant k in the range from 0.2 to 3 is changed. In this variant, 11 simulations for straight flight and 11 simulations for flight with maneuver were performed. The simulation results are shown in Figure 7.

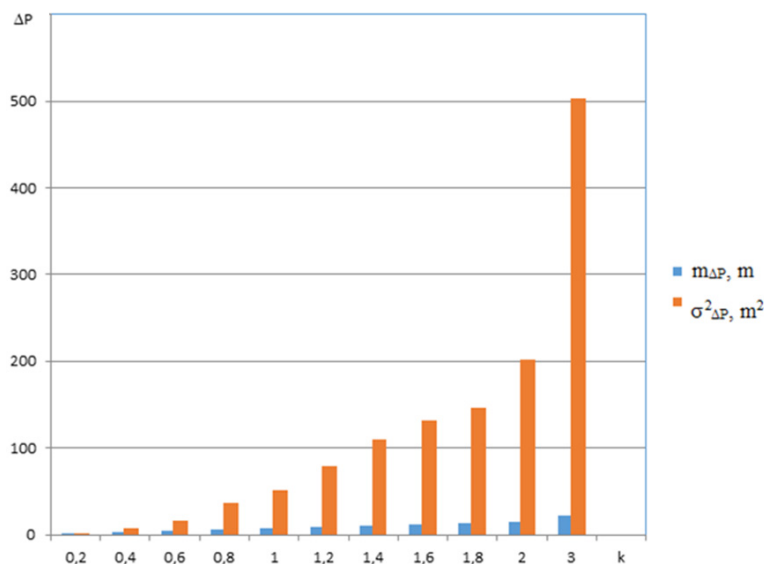


Figure 7. Accuracy of ACS positioning for straight flight.

Figure 7 shows the mean values $m_{\Delta P}$ and dispersions $\sigma^2_{\Delta P}$ of ACS positioning errors for straight flight. The mean ACS positioning error values range from 1.45 m to 21.67 m. Dispersions of ACS $\sigma^2_{\Delta P}$ positioning errors range from 1.94 m² to 503.23 m². The results of the ACS positioning accuracy simulation confirmed that the ACS positioning errors depend on the accuracy of the distance measurement from FOs to the ACS d_{1-4} , according to which the ACS determines its position. The accuracy of the proposed system meets the requirements that are placed on such devices.

Figure 8 shows the mean values $m_{\Delta P}$ and dispersions $\sigma^2_{\Delta P}$ of ACS positioning errors for the maneuvered flight. The mean ACS positioning error values range from 2.04 m to 32.1 m. Dispersions of ACS $\sigma^2_{\Delta P}$ positioning errors range from 3.2 m² do 857.22 m². In addition, in this case, the results of the ACS positioning accuracy simulation confirmed that the ACS positioning errors depend on the accuracy of the distance measurement d_{1-4} . The simulation results showed that the accuracy of the proposed ACS deteriorated. Assuming that this is due to a more significant change in the geometry of the system that occurs during the maneuver flight simulation, some simulations were performed using a combination of precisely measured distances of individual FO₁₋₄ from the ACS and pseudo-distances. They were burdened with errors to determine the position of the ACS. Initial conditions for FOs were the same as in previous simulations. FO₁₋₄ coordinate errors were generated by generators under the same conditions as in previous simulations. The constant k was equal to 1. Simulations were performed for a straight flight with a flight duration of 1375 s. The results of all performed simulations are shown in Figure 9.

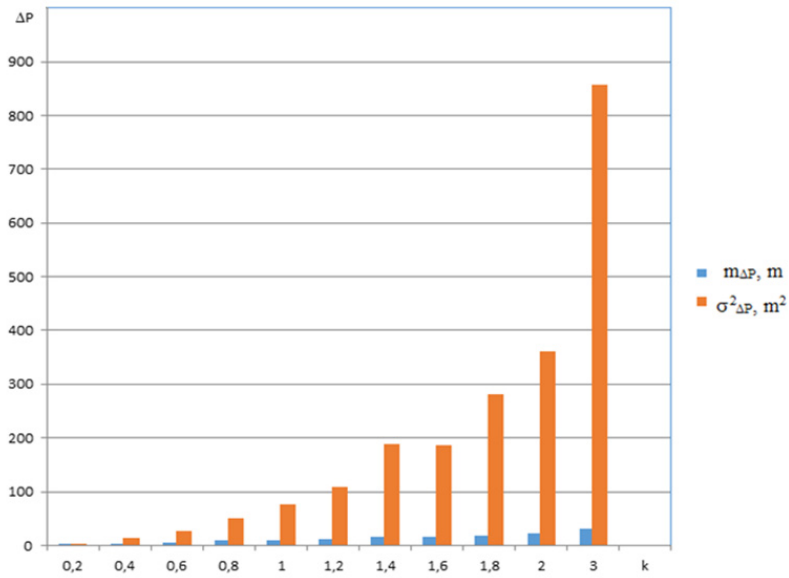


Figure 8. Accuracy of ACS positioning accuracy for maneuvered flight.

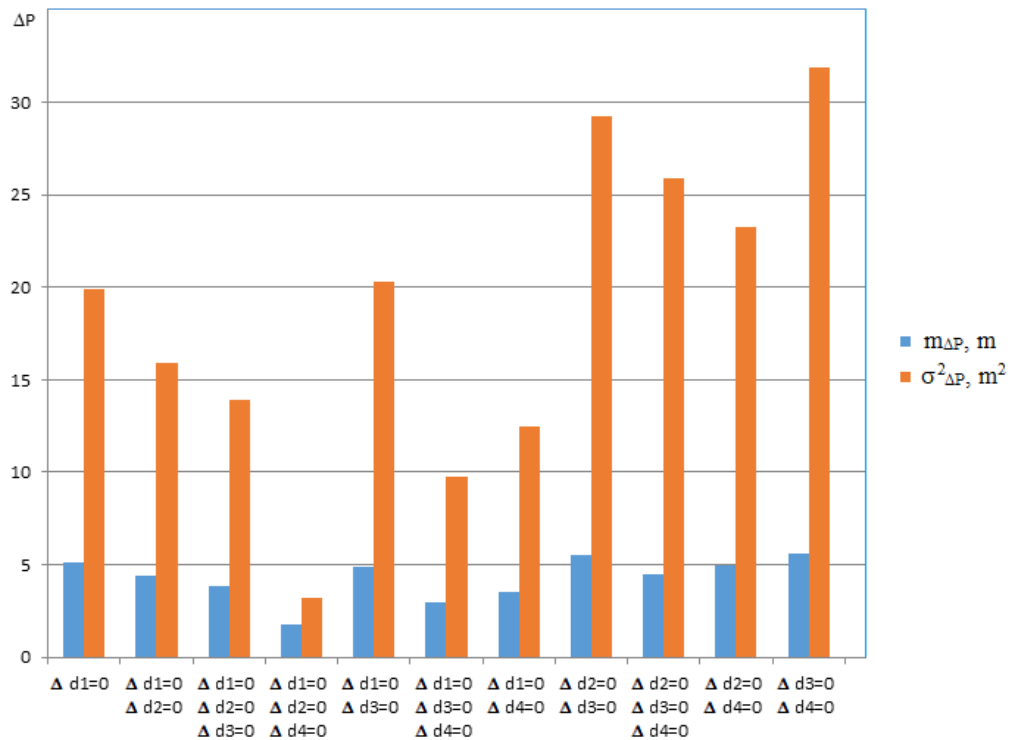


Figure 9. Accuracy of ACS positioning for straight flight and various distance measurement: errors Δd_1 – Δd_4 .

The results of the simulation show that the mean values of the ACS positioning errors and the dispersion of the ACS positioning errors were smaller than if $\Delta d_{1-4} \neq 0$. The best improvement occurred with the combination $\Delta d_1 = 0, \Delta d_2 = 0, \Delta d_4 = 0$, and $\Delta d_3 \neq 0$, where the mean value of the positioning error ACS was equal to 1.81 m and the dispersion of the positioning error ACS was equal to 3.18 m². The simulation results confirm that the time synchronization requirements of individual network users are high and inaccurate parameters in the transmitted message from individual FOs directly affect the accuracy of ACS positioning. Additional simulations were performed with the change of FO₁₋₄

position relative to the ACS. When selecting the initial coordinates of the FOs, we placed the individual users due to the geographical course of the LOT5MF flight, on which the ACS is located. The geographical course of the flight LOT5MF was equal to 345° . The geographical course of RJA39K was 74° , the geographical course of FHM6112 was 255° , the geographical course of LOT653 was 173° , and the geographical course of WZZ3007 was 160° . We gradually changed the distances of individual FOs from the ACS in the range of 10 to 50 km. Selected simulation results are shown in Figure 10.

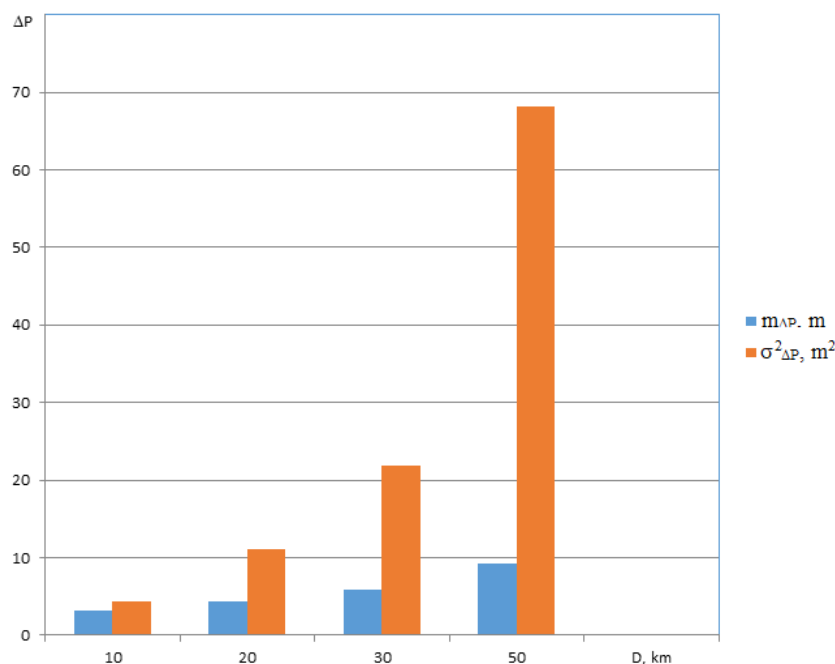


Figure 10. Accuracy of ACS positioning for selected positions FOs, straight flight.

Figure 10 shows that as the distances of FOs RJA39K, FHM6112, LOT653, and WZZ3007 from the ACS increase, the ACS positioning errors increase. On this basis, the accuracy of ACS positioning depends on the relative position of network users. The simulation results confirmed that the proposed ACS determines its position concerning other network users with the required accuracy to a distance of at least 50.0 km.

5. Conclusions

The main contribution of this paper is that we derived algorithms for the operation of an anti-collision system for small civil aircraft, and also designed movement trajectory models of five flying objects which operate within the aviation communication network. Movement trajectories of the FOs were modeled in a geocentric coordinate system. Based on the acquired algorithms and models of FO trajectories, a simulation of the operation of an anti-collision system for small civil aircraft was carried out. During the simulation, it was assumed that flying objects RJA39K, FHM6112, LOT653, WZZ3007, and LOT5MF operate in the communication network of aviation. The LOT5MF is a small civil aircraft equipped with an onboard anti-collision system. Using the anti-collision system, it establishes its position based on the data received from the aforementioned flying objects. The Matlab software was used to carry out the computer simulation. The accuracy of determining the position of a flying object LOT5MF with an anti-collision system depending on the errors of the position data of flying objects RJA39K, FHM6112, LOT653, WZZ3007 was investigated. The errors of the coordinates of the flying objects were simulated by the constant k , the value of which was modified from 0 (no error) up to 3 (maximum error). The simulation results prove that the precision of position identified by the anti-collision system in the model simulation presented in Figure 7, with the constant k ranging from 0.1 to 3.0,

varied (dispersions $\sigma^2_{\Delta P}$ of ACS positioning errors) from 1.94 m² to 503.23 m². During the flight with the maneuver, the positioning error of the anti-collision system was greater. See Figure 8. Based on the acquired simulation results relating to the presented model situations, it can be concluded that it is possible to apply the anti-collision system designed onboard small civil aircraft. The accuracy of positioning by the anti-collision system onboard LOT5MF depending on the mutual positions of flying objects RJA39K, FHM6112, LOT653, WZZ3007 was verified using the simulation. Deriving from the simulation results presented in Figure 10 can be stated that the anti-collision system identified its position with the errors depending on its distance from individual FOs. Modifying the distance between the anti-collision system and individual FOs from 10.0 km to 50.0 km, the errors of position identification were ranging from (dispersions $\sigma^2_{\Delta P}$ of ACS positioning errors) 4.29 m² to 68.25 m². This fact confirms that the designed anti-collision system is operational in establishing its position against other FOs, with the distance from the given FOs being 50.0 km maximum. This can be explained by the fact that the anti-collision system's position is established by a distance-measuring method. The advantage of the anti-collision system is that it is independent of satnav systems and secondary radars. The disadvantage of the proposed anti-collision system is that it identifies its position only with those flying objects that are part of the air communication network. On the other hand, the essential advantage of this system is its low price. As stated in [23], the average root-mean-square error (RMSE) proposed by the system ADS-B (Automatic Dependent Surveillance-Broadcast)/MLAT (Multilateration Surveillance) data fusion framework is 15.3 m compared to the average RMSE of ADS-B which is 30 m. ADS-B is directly dependent on GNSS (Global Navigation Satellite System). Based on this, we can say that the accuracy of the anti-collision system is better.

Author Contributions: Conceptualization, M.D. and P.D.; data curation, M.D.; methodology, L.M., formal analysis, P.D. and L.M.; validation M.D. and P.D.; supervision, L.M. and P.D.; resources, M.D. and P.D.; writing—original draft preparation, M.D. and P.D.; writing—review and editing, L.M. All authors have read and agreed to the published version of the manuscript.

Funding: All authors agree to the final version.

Institutional Review Board Statement: Not applicable.

Informed Consent Statement: All authors agree to the final version.

Data Availability Statement: Not applicable.

Acknowledgments: Not applicable.

Conflicts of Interest: The authors declare no conflict of interest.

References

1. Džunda, M.; Dzurovcin, P.; Kavka, P. Utilizing the principle of relative navigation in anti-collision systems. In Proceedings of the International Scientific Conference on Modern Safety Technologies in Transportation (MOSATT), Kosice, Slovakia, 28–29 November 2019; pp. 39–44.
2. Džunda, M.; Dzurovcin, P.; Koščák, P.; Liptáková, D. Relative navigation in anti-collision systems for UAV. In Proceedings of the International Scientific Conference on Modern Safety Technologies in Transportation (MOSATT), Kosice, Slovakia, 28–29 November 2019; pp. 44–48.
3. Džunda, M.; Dzurovcin, P.; Cekanova, D. Operational economic aspects of warning collision systems for helicopters. In Proceedings of the 22nd International Scientific Conference on Transport Means, Trakai, Lithuania, 3–5 October 2018; pp. 1151–1155, PTS I–III.
4. Beinarovica, A.; Gorobetz, M.; Levchenkov, A. Control algorithm of multiple unmanned electrical aerial vehicles for their collision prevention. In Proceedings of the 12th International Conference on Intelligent Technologies in Logistics and Mechatronics Systems (ITELMS), Panevezys, Lithuania, 26–27 April 2018; pp. 37–43.
5. Graffstein, J. Functioning of an air anti-collision system during the test flight. *Aviation* **2014**, *18*, 44–51. [[CrossRef](#)]
6. Wang, Z.; Yu, B.; Chen, J.; Liu, C.; Zhan, K.; Sui, X.; Xue, Y.; Li, J. Research on lidar point cloud segmentation and collision detection algorithm. In Proceedings of the 6th International Conference on Information Science and Control Engineering (ICISCE), Shanghai, China, 20–22 December 2019; pp. 475–479. [[CrossRef](#)]

7. Lee, R.C.; Chen, B.H. Building an UAV anti-collision system with low-power FM ranging radar and camera image. In Proceedings of the 2019 IEEE Eurasia Conference on IOT, Communication and Engineering (ECICE), Yunlin, Taiwan, 3–6 October 2019; pp. 387–389. [CrossRef]
8. Bascetta, L.; Magnani, G.; Rocco, P.; Migliorini, R.; Pelagatti, M. Anti-collision systems for robotic applications based on laser time-of-flight sensors. In Proceedings of the IEEE/ASME, International Conference on Advanced Intelligent Mechatronics, Montreal, QC, Canada, 6–9 July 2010; pp. 278–284. [CrossRef]
9. Lee, H.W.; Zhu, Y.; Shi, X.; Peng, F.F.; Jin, W.J. Research of four-axis aircraft using WIFI and rotary anti-collision system. In Proceedings of the 2018 IEEE International Conference on Applied System Invention (ICASI), Tokyo, Japan, 13–17 April 2018; pp. 665–668. [CrossRef]
10. Zanobini, A. A drone anti-collision system: Maintaining a fixed distance from a target during the flight. In Proceedings of the 2016 18th Mediterranean Electrotechnical Conference (MELECON), Limassol, Cyprus, 16–20 April 2016; pp. 1–6. [CrossRef]
11. Brcko, T.; Androjna, A.; Srše, J.; Boć, R. Vessel multi-parametric collision avoidance decision model: Fuzzy approach. *J. Mar. Sci. Eng.* **2021**, *9*, 49. [CrossRef]
12. Fu, H.; Cui, B.; Zhuang, B.; Zhang, J. Anti-collision and obstacle avoidance of mobile sensor-plus-actuator networks over distributed parameter systems with time-varying delay. *Int. J. Control Autom. Syst.* **2021**, *19*, 2373–2384. [CrossRef]
13. Tarazona, R.D.F.; Lopera, F.R.; Sánchez, G.D.G. Anti-collision system for indoors quadcopter navigation using fuzzy controllers and range sensors. *Rev. Investig. Univ. Quindío* **2016**, *28*, 101–108.
14. Tarazona, R.D.F.; Lopera, F.R.; Sánchez, G.D.G. Anti-collision system for navigation inside an UAV using fuzzy controllers and range sensors. In Proceedings of the XIX Symposium on Image, Signal Processing and Artificial Vision (STSIVA), Armenia, Colombia, 17–19 September 2014.
15. Gorobetz, M.; Ribickis, L.; Levchenkov, A.; Beinarovica, A. Machine learning algorithm of immune neuro-fuzzy anti-collision embedded system for autonomous unmanned aerial vehicles team. In Proceedings of the 2nd International Conference on Applications of Intelligent Systems (APPIS), Las Palmas de Gran Canaria, Spain, 7–9 January 2019.
16. Beinarovica, A.; Gorobetz, M.; Levchenkov, A. Self-organized learning algorithm for immune neuro-fuzzy anti-collision system of autonomous unmanned aerial vehicles' team. In Proceedings of the 22nd International Scientific Conference on Transport Means (Transport Means), Trakai, Lithuania, 3–5 October 2018; pp. 1334–1341.
17. Liu, Y.; Liang, Y.; Li, K. Anti-collision cooperative control strategy for multi-agent based on collision probability. In Proceedings of the 4th International-Academy-of-Astronautics Conference on Dynamics and Control of Space Systems (DyCoSS '2018), National University of Defense Technology, Changsha, China, 21–23 May 2018; Book Series: Advances in the Astronautical Sciences. 2018; Volume 165, pp. 199–207. Available online: <https://www.univelt.com/linkedfiles/v165%20Contents.pdf> (accessed on 1 January 2022).
18. Visual Scanning Technique. Available online: <https://skybrary.aero/articles/visual-scanning-technique> (accessed on 1 January 2022).
19. Improved Ground Collision Avoidance System (DRC-TOPS-19). Available online: <https://technology.nasa.gov/patent/DRC-TOPS-19> (accessed on 1 January 2022).
20. Vosecký, S. *Radionavigace. Učební Texty pro Teoretickou Přípravu Dopravních Pilotů dle Předpisu JAR-FCL-1*; CERM: Brno, Slovakia, 2011; ISBN 9788072047642.
21. Džunda, M.; Kotianová, N.; Dzurovčin, P.; Szabo, S.; Jenčová, E.; Vajdová, I.; Koščák, P.; Liptáková, D.; Hanák, P. Selected aspects of using the telemetry method in synthesis of RelNav system for air traffic control. *Int. J. Environ. Res. Public Health* **2020**, *17*, 213. [CrossRef] [PubMed]
22. Džunda, M. Modeling of the flight trajectory of flying objects. In Proceedings of the NTAD 2018—13th International Scientific Conference—New Trends in Aviation Development, Kosice, Slovakia, 30–31 August 2018; pp. 132–136.
23. El Marady, A.A.W. Enhancing accuracy and security of ADS-B via MLAT assisted-flight information system. In Proceedings of the 2017 12th International Conference on Computer Engineering and Systems (ICCES), Cairo, Egypt, 19–20 December 2017; pp. 182–187. [CrossRef]